Biophysical Journal Volume 76 March 1999 1280–1292

The Forward Rate of Binding of Surface-Tethered Reactants: Effect of Relative Motion between Two Surfaces

Kai-Chien Chang and Daniel A. Hammer
School of Chemical Engineering, Cornell University, Ithaca, New York 14853 USA

ABSTRACT The reaction of molecules confined to two dimensions is of interest in cell adhesion, specifically for the reaction between cell surface receptors and substrate-bound ligand. We have developed a model to describe the overall rate of reaction of species that are bound to surfaces under relative motion, such that the Peclet number is order one or greater. The encounter rate between reactive species is calculated from solution of the two-dimensional convection-diffusion equation. The probability that each encounter will lead to binding depends on the intrinsic rate of reaction and the encounter duration. The encounter duration is obtained from the theory of first passage times. We find that the binding rate increases with relative velocity between the two surfaces, then reaches a plateau. This plateau indicates that the increase in the encounter rate is counterbalanced by the decrease in the encounter duration as the relative velocity increases. The binding rate is fully described by two dimensionless parameters, the Peclet number and the Damköhler number. We use this model to explain data from the cell adhesion literature by incorporating these rate laws into "adhesive dynamics" simulations to model the binding of a cell to a surface under flow. Leukocytes are known to display a "shear threshold effect" when binding selectin-coated surfaces under shear flow, defined as an increase in bind rate with shear; this effect, as calculated here, is due to an increase in collisions between receptor and ligand with increasing shear. The model can be used to explain other published data on the effect of wall shear rate on the binding of cells to surfaces, specifically the mild decrease in binding within a fixed area with increasing shear rate.

GLOSSARY

a	encounter radius
C_∞	substrate surface ligand concentration
D	relative diffusion coefficient
D_1, D_2	surface diffusivity of receptor and ligand
L	view length
L_c	radius of the contact region
E	activation energy for reaction
F_s	steric factor
H_c	cut-off distance to define a reactive contact region
h	separation distance between plate and cell
k_o	perfect sink forward rate constant
k_f	intrinsic association rate constant
k_{in}	intrinsic reaction rate constant
k_{ad}	observable adhesion rate constant
N_r	number of receptors in contact region
Nu	Nusselt number
P	capture probability
Pe	Peclet number
R	cell radius
U	translational velocity of cell
$\mathbf{V}$	relative velocity of the two surfaces

Greek symbols

δ	Damköhler number
Λ	dimensionless encounter duration
ν	vibrational frequency during encounter
τ	encounter duration
Ω	angular velocity of cell

INTRODUCTION

The reaction of molecules confined to two dimensions is of interest in adhesion, tribology, and thin-film catalysis. The adhesion between two surfaces where the interfacial force is mediated by adhesive macromolecules (ligands and receptors) on two surfaces can be found in many biological processes that depend on cell adhesion, including thrombus formation (Mustard et al., 1978), the inflammatory response (Harlan, 1975; Osborn, 1990), lymphocyte homing (Berg et al., 1989), cancer cell metastasis (Nicolson, 1988), and cell-mediated immune reactions (Springer, 1990). Cell adhesion requires first close contact between two cell surfaces and then a biochemical reaction that leads to the formation of tethers to link the two surfaces. In many cases, cell adhesion occurs under conditions of flow in which one or both cells are in motion. During close contact, there may be a relative motion between two surfaces, and the magnitude of this relative motion depends on the solutions of the equations of motion for the cells and intervening fluid. The effect of this relative motion on the overall rate of binding between receptor and ligand is the main subject of this article.

The binding between a cell-bound receptor and tethered ligand under flow is mathematically similar to the binding between a free ligand and a cell-bound receptor in the presence of convective flow. Existing theories (Purcell,

Received for publication 21 May 1997 and in final form 23 November 1998.

Address reprint requests to Dr. Daniel A. Hammer, Department of Chemical Engineering, University of Pennsylvania, 392 Towne Bldg., 220 S. 33rd St., Philadelphia, PA 19104. Tel.: 215-573-6761; Fax: 215-573-2093; E-mail: hammer@seas.upenn.edu.

0006-3495/99/03/1280/13 $2.00

1978; Brunn, 1981; Glaser, 1993; Model and Omann, 1995) focus mainly on solving the concentration profile for the ligand molecules near the cell surface. This mathematical approach may also be used to analyze the binding of solution ligands to surface-bound receptors in diagnostic devices, such as the BIAcore machine (Myszka et al., 1998). For the cases where the cell surfaces are partially reactive (owing to the partial coverage of the cell surface by receptors and finite reactivity of cell surface receptors), these theories adopt the boundary condition that the net flux into the surface is equal to the rate of reaction at the surface. In these calculations, it has been assumed that the rate of binding is first order in the local ligand concentration near the cell, and that the intrinsic association rate constant between receptors and ligands is independent of flow. This type of partially absorbing boundary condition was first proposed by Collins and Kimball (1949). However, the Collins-Kimball treatment does not allow for the possibility that the association rate constant depends on the relative velocity of the reactants. Because the residence time needed for a ligand to stay sufficiently close to a surface-bound receptor decreases with increasing velocity, the rate of transport may affect the "reactivity" of receptor and ligand, and thus the Collins-Kimball boundary condition is not sufficiently robust for this problem. In the case of a solvated ligand binding to a cell surface receptor, the relative velocity between a ligand and the surface will likely not affect the probability of reaction, owing to the no-slip boundary condition for a fluid near a surface (Brunn, 1981). However, in the case where receptors and ligands are both tethered to surfaces, the relative motion between ligands and receptors is dictated by the motion of the surfaces. For a sphere in shear flow near a wall in the low Reynolds number flow, solution of Stokes equations indicates a substantial slip velocity between the particle and the surface (Goldman et al., 1967). Thus with respect to wall-attached ligand, the sphere-tethered receptors in the region of contact should have a higher relative velocity than free stream ligands at the same flow condition. To determine the effect of this relative velocity on binding, we should compare its magnitude with the lateral diffusivity of receptors. Defining a Peclet number Pe by (radius of the receptor)(relative velocity)/(lateral diffusivity), we can estimate the ratio of convection to diffusion. For a typical cell size of 10 μm, the relative slip velocity at a shear rate of 60–200 1/s is ~0.4–1.3 cm/min (Goldman et al., 1967). Given typical values for the lateral diffusivity (10^{-10} cm^2/s) and radius of the receptor (10^{-7} cm), the Peclet number is ~6–20. This indicates that the convection should be important—in fact, dominant—in affecting the rate of binding for surface-bound receptors.

Previous theoretical studies (Xia et al., 1993) have concentrated on the effects of flow on the collision rate between cells and a glass surface. Little attention has been paid to the microscopic factors that control receptor-ligand binding kinetics after the collision. Potanin and colleagues did include the relative velocity in their rate expression to model cell coagulation (Potanin et al., 1993). However, their estimation of the rate of formation of encounter complexes is a sum of the contribution from convection (high Pe) and the one from diffusion (low Pe). For cases where Pe is O(1–10), the estimation obtained by superposition is not likely to be correct. In performing calculations with convection-dependent reaction rate, terms that depend on the relative velocity between surfaces are suppressed (Potanin et al., 1993). Thus the effect of relative motion on close-contact duration cannot be revealed from their work. Our work represents an improvement over this approach, as we explicitly calculate the effect of Pe on the rate of reaction and incorporate this dependency into calculations of adhesion.

It is common to use flow chamber assays to study adhesion mediated by cell surface receptors (Lawrence and Springer, 1991; Tempelman and Hammer, 1994; Goetz et al., 1994; Brunk et al., 1996; von Andrian et al., 1995; Finger et al., 1996). In selectin systems, a curious phenomenon called the "shear threshold effect" has recently been elucidated (Finger et al., 1996). In it, the rate of tether formation between the traveling cell and the ligand-coated surface appears to increase with shear rate up to a critical value of shear rate, then decreases with further increases in shear rate. The seemingly perplexing aspect of the shear threshold effect is the increase in attachment rate with shear rate. In this paper, we explain that increasing shear rate leads to an increase in the rate of encounter between receptor and ligand, up to a maximum at which the collision rate equals the departure rate. Thus if the reaction between receptor and ligand is controlled by transport, then one should see an increase in binding with shear at low shear rates, precisely as is seen in the shear threshold effect (Finger et al., 1996).

In systems that display firm adhesion, most of the data on adhesion as a function of fluid velocity indicate that the extent of cell attachment decreases with fluid velocity (Lawrence et al., 1990; Lawrence and Springer, 1991; Luscinskas et al., 1994; Tempelman and Hammer, 1994; Melder et al., 1995; Moore et al., 1995; Swift et al., 1998). The extent of cell attachment involves factors such as the intrinsic rate of association between cell surface receptors and substrate ligand, as well as the size of the field of microscopic observation and the relative velocity of surfaces. Because the extent of adhesion only partially depends upon the intrinsic association rate, one should not conclude that the intrinsic rate of association between molecules decreases with increasing fluid velocity. As the fluid flow rate increases, the time needed for each cell to pass through the field of view decreases, and the duration of encounter must be taken into account in determining the intrinsic association rate. Furthermore, measurements of the levels of association from the net number of cells bound must take into consideration dissociation of cells from surfaces, which contributes to the total mass balance of binding.

We find that most experiments designed to measure the intrinsic association rate, including our own (Tempelman and Hammer, 1994), have not properly taken these factors

into account (Pierres et al., 1994; Finger et al., 1996). This failure comes from two sources: 1) failing to account for the decrease in transit time through a fixed field of view as the flow rate increases, and 2) failing to properly account for the rate of encounter between receptors and ligands when a cell is moving relative to a fixed surface. In this paper, we correct these deficiencies, which will provide a basis for the improved interpretation of experimental data. In addition, we improve adhesive dynamics, a simulation method for cell adhesion (Hammer and Apte, 1992), by incorporating into the method the proper expression for the rate of binding as a function of fluid velocity. The net effect of our effort is a more accurate quantitative understanding of cell attachment under flow.

THEORY

Fig. 1 illustrates the coordinate system that governs our calculation. Conceptually, surface 2 is a ligand-coated substrate, and surface 1 is the bottom surface of a receptor-coated cell. We model receptor-ligand binding as a two-step process, requiring encounter and reaction. During the encounter, two molecules are brought to adjacent positions. After the encounter, the molecules react, which involves quasivibrational adjustments of receptor and ligand configurations and is assumed to be independent of transport. The collision (transport) is caused by the relative motion of surfaces and the lateral diffusion of each molecule on the surfaces. We can determine the encounter rate by solving the convection-diffusion equation with appropriate boundary conditions. We choose an arbitrary receptor on the cell (surface 1) as our target molecule and locate the origin of our coordinate system at this molecule. The separation distance between these two surfaces is sufficiently small that the molecules on both sides can react with each other. With respect to this target receptor, ligands on surface 2 behave as if they are under convective motion with a constant velocity **V**. In addition, the reactive molecules may diffuse on their surfaces; for example, the receptors on surface 1 may diffuse in the plane of the membrane. Because the ligands and receptors are restricted to parallel surfaces, this problem is two-dimensional. Therefore the concentration, $C(\mathbf{r})$, of ligand molecules on surface 2 at $\mathbf{r}$ relative laterally to the position of the target receptor is assumed to satisfy a 2-D convection-diffusion equation,

$$D\nabla^2 C(\mathbf{r}) - \mathbf{V}\cdot\nabla C(\mathbf{r}) = 0 \tag{1}$$

where D is the relative diffusion coefficient, equaling to the sum of the surface self-diffusivities D_1 and D_2 for the target receptor and ligand, respectively.

Applying the Smoluchowski theory (1917), the flux J through the reactive circle of radius a corresponding to a cell surface receptor is related to the forward rate constant for encounter, k_o, as

$$J = k_o C_\infty \tag{2}$$

where C_∞ is the average surface concentration of ligand.

We first calculate the flux that includes any particle reaching separation distance a for the first time. This is equivalent to assigning a perfect sink condition on the boundary $r = a$ (appropriate for calculating the encounter rate). With boundary conditions

$$C(r) = C_\infty \quad \text{at } r = \infty \tag{3}$$

$$C(r) = 0 \quad \text{at } r = a, \tag{4}$$

The dimensionless flux can be described in dimensionless form as the Nusselt number, $\mathrm{Nu} = J/\pi D C_\infty$,

$$\mathrm{Nu} = 2\left[\frac{I_0(\mathrm{Pe}/2)}{K_0(\mathrm{Pe}/2)} + 2\sum_{n=1}^{\infty}(-1)^n \frac{I_n(\mathrm{Pe}/2)}{K_n(\mathrm{Pe}/2)}\right] \tag{5}$$

where Pe is the Peclet number defined as $|\mathbf{V}|a/D$, and I_n, K_n are modified Bessel functions of the second kind. We plot Nu as a function of Pe in Fig. 2. From Eq. 2 and the definition of Nu, the perfect sink forward rate constant is given by $k_o = \pi D\mathrm{Nu}$, with Nu given by the solution of Eq.

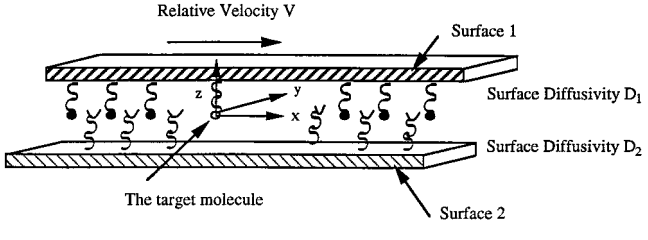

FIGURE 1 Schematic diagram of the system. The target molecule (*open circle*) is chosen to be on surface 1 and as the origin of the coordinate system. Molecules on surface 1 and surface 2 are assumed to have lateral Brownian motion, which is characterized by diffusion coefficients D_1 and D_2, respectively. The two surfaces move parallel to each other with a relative velocity V.

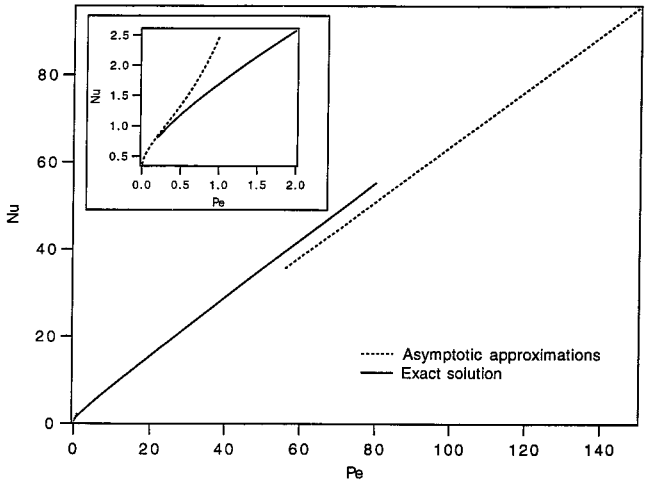

FIGURE 2 The calculated Nusselt number as a function of the Peclet number. The solid curve corresponds to the numerical values of Eq. 5; the dashed curves correspond to asymptotic approximations at low and high Pe. The inset gives a clear view at low Pe.

2. Fig. 2 indicates that the first encounter rate increases with the relative velocity of the two surfaces. For the case where $Pe \ll 1$, Nu is given asymptotically as $2/(\ln(4/Pe) - \gamma)$, where γ is Euler's constant, 0.577. . . Careful consideration must be given to the case where there is no convection ($\mathbf{V}$ or $Pe = 0$). In this limit, the encounter is controlled purely by diffusion and Nu is given, $Nu = 2/\ln(b/a)$ (DeLisi, 1980; Lauffenburger and Linderman, 1993), where b is one-half of the mean distance between ligand. This alternative expression should be used to describe the encounter when $Pe \ll 1$. For example, when $b/a = 10$, the valve of Pe that makes Nu obtained from Eq. 5 equal to $2/\ln(b/a)$ is 0.2. Therefore as $Pe < 0.2$, Nu should be the constant obtained from the expression $2/\ln(b/a)$. When $Pe \gg 1$, the asymptotic value of Nu is $2Pe/\pi$. As one would expect, the encounter rate increases linearly with relative velocity. The asymptote at high Pe displayed in Fig. 2 shows a poor agreement with values calculated from Eq. 5. From scaling analysis, the next correction term of the asymptotic approximation is $O(Pe^{1/3})$, which represents a significant factor as Pe increases. This explains the discrepancy between the exact and asymptotic solutions at high Pe.

Because not every encounter leads to binding, we need to obtain the probability P that a colliding receptor-ligand pair will ultimately react. To calculate P, we assume that during each encounter the target receptor will take the reaction position and establish meaningful collisions at any position inside the reactive circle ($r = a$) with equal probability. After the encounter, the fate of the engaged ligand will be either to bind the target receptor or to pass over it. Therefore P is the probability that a binding event occurs before the ligand has left the circle. Here we use the formula

$$P = k_{in}/(k_{in} + 1/\tau) \tag{6}$$

to approximate this probability (Moore and Pearson, 1981), where τ is the averaged duration of an encounter and k_{in} is the probability, per unit time, that a nearby receptor-ligand pair will lead to binding. This is the intrinsic reaction rate, which depends upon the vibrational motion of the receptor and ligand, which occurs at a frequency ν. Reaction occurs when the vibrational energy exceeds the activation energy for reaction, E. Thus the intrinsic rate k_{in} is given as $\nu F_s e^{-E/kT}$, where F_s is a steric factor and kT is the thermal energy. Because k_{in} is assumed not to depend on relative motion, we treat it as a constant in our analysis.

There are limits in which Eq. 6 may not strictly apply. The inverse of the frequency ν indicates the minimum time of close proximity for two molecules needed for a reaction to occur. Therefore if the maximum duration time, i.e., $2a/|\mathbf{V}|$, is less than $1/\nu$, the probability P should equal zero identically. This corresponds to the case where the relative velocity is so high that not a single binding event can happen, regardless of the observation time. However, the general dynamic feature that $P \to 0$ as $k_{in} \to 0$ is retained in Eq. 6.

To obtain P, next we need to calculate the duration of each encounter τ. The first passage time approach (Szabo et al., 1980; Gardiner, 1990) gives the average time, $T(\mathbf{r})$, needed for a particle initially at position $\mathbf{r}$ inside a certain region to reach the boundary for the first time. Because we have assumed that collisions could occur at any location inside the circle of radius a surrounding the receptor, τ is the mean value of $T(\mathbf{r})$, where one takes the average over the circle. We neglect changes in duration caused by molecules reentering the region and focus on the escape of a single molecule. To obtain $T(\mathbf{r})$ by the first passage time approach, we start from the backward Fokker-Planck equation,

$$\frac{\partial p(\mathbf{r}', t|\mathbf{r}, 0)}{\partial t} = \mathbf{V} \cdot \nabla_r p(\mathbf{r}', t|\mathbf{r}, 0) + D\nabla_r^2 p(\mathbf{r}', t|\mathbf{r}, 0), \tag{7}$$

where $p(\mathbf{r}', t|\mathbf{r}, 0)$ is the conditional probability density function, which denotes the probability of the particle being at position $\mathbf{r}'$ given that it is at $\mathbf{r}$ at $t = 0$. Then with an absorbing boundary condition to characterize the disappearance of the particle from the disk, i.e., $p(\mathbf{r}', t|\mathbf{r}, 0) = 0$ at $|\mathbf{r}| = a$, Eq. 7 gives the probability that a particle will not leave the circle in a time t. Thus the probability $W(\mathbf{r}, t)$ that the particle is still inside the circle at time t is

$$W(\mathbf{r}, t) = \int_{|\mathbf{r}'|<a} p(\mathbf{r}', t|\mathbf{r}, 0)\mathrm{d}\mathbf{r}'. \tag{8}$$

Integrating Eq. 7 with respect to $\mathbf{r}'$, one finds that $W(\mathbf{r}, t)$ satisfies the equation

$$\frac{\partial W(\mathbf{r}, t)}{\partial t} = \mathbf{V} \cdot \nabla_r W(\mathbf{r}, t) + D\nabla_r^2 W(\mathbf{r}, t), \tag{9}$$

with the initial condition $W(\mathbf{r}, 0) = 1$ and the boundary condition $W(\mathbf{r}, t) = 0$ at $|\mathbf{r}| = a$. Now let the time when the particle leaves the circle starting at $\mathbf{r}$ be $T(\mathbf{r})$. Notice that the event $\{T(\mathbf{r}) > t\}$ takes place if and only if the particle is still inside the circle at time t; thus,

$$P\{T(\mathbf{r}) > t\} = W(\mathbf{r}, t). \tag{10}$$

Now we can compute the mean of $T(\mathbf{r})$, *namely, the mean first passage time*,

$$\langle T(\mathbf{r})\rangle = -\int_0^\infty t\frac{\partial W(\mathbf{r}, t)}{\partial t}\,\mathrm{d}t. \tag{11}$$

After integration by parts, it can be shown that

$$\langle T(\mathbf{r})\rangle = \int_0^\infty W(\mathbf{r}, t)\mathrm{d}t. \tag{12}$$

Hence, by further integrating Eq. 9 with respect to time, we obtain the differential equation

$$\mathbf{V} \cdot \nabla_r\langle T(\mathbf{r})\rangle + D\nabla_r^2\langle T(\mathbf{r})\rangle = -1 \tag{13}$$

with the boundary condition $\langle T(\mathbf{r})\rangle = 0$ at $|\mathbf{r}| = a$. Similar to the methods used for solving Eq. 1 (see Appendix A), the solution for Eq. 13 in polar coordinates is

$$\langle T(r,\theta)\rangle = \exp(-\kappa r\cos\theta)\sum_{n=0}^{\infty} A_n I_n(\kappa r)\cos n\theta - \frac{r\cos\theta}{|\mathbf{V}|} \tag{14}$$

where $\kappa = |\mathbf{V}|/2D$, I_n is the modified Bessel function of the second kind, and A_n's are

$$A_0 = \frac{a}{|\mathbf{V}|}\frac{I_1(\kappa a)}{I_0(\kappa a)} \tag{15}$$

$$A_n = \frac{a}{|\mathbf{V}|}\frac{I_{n-1}(\kappa a) + I_{n+1}(\kappa a)}{I_n(\kappa a)} \quad \text{for } n > 0. \tag{16}$$

Hence, the average duration of an encounter is

$$\tau = \frac{\int_{|r|\le a}\langle T(r,\theta)\rangle r\,\mathrm{d}r\,\mathrm{d}\theta}{\pi a^2}$$

$$= \frac{a}{|\mathbf{V}|}\left(\frac{-I_1(\kappa a)^3}{I_0(\kappa a)} + \sum_{n=1}^{\infty}(-1)^{n+1}\frac{I_{n-1}(\kappa a)I_{n+1}(\kappa a)(I_{n-1}(\kappa a) + I_{n+1}(\kappa a))}{I_n(\kappa a)}\right) \tag{17}$$

We also obtain the values of τ for two limiting values of Pe. When Pe $\ll 1$, $\tau \sim a^2/8D$. As Pe $\gg 1$, $\tau \sim 8a/3|\mathbf{V}|\pi$. Now introducing a dimensionless duration time, Λ:

$$\Lambda = \tau/(a^2/D)$$

$$\Lambda = \frac{1}{\mathrm{Pe}}\left(\frac{-I_1(\mathrm{Pe}/2)^3}{I_0(\mathrm{Pe}/2)} + \sum_{n=1}^{\infty}(-1)^{n+1}\frac{I_{n-1}(\mathrm{Pe}/2)I_{n+1}(\mathrm{Pe}/2)(I_{n-1}(\mathrm{Pe}/2) + I_{n+1}(\mathrm{Pe}/2))}{I_n(\mathrm{Pe}/2)}\right) \tag{18}$$

Thus Λ is a function of Pe only. We plot Λ as a function of Pe in Fig. 3.

Defining a dimensionless Damköhler number, $\delta = a^2 k_{in}/D$, we can express the probability of binding, P, as

$$P = \Lambda\delta/(1 + \Lambda\delta) \tag{19}$$

The effective reaction rate then becomes

$$k_f = k_o P = \pi D\mathrm{Nu}P. \tag{20}$$

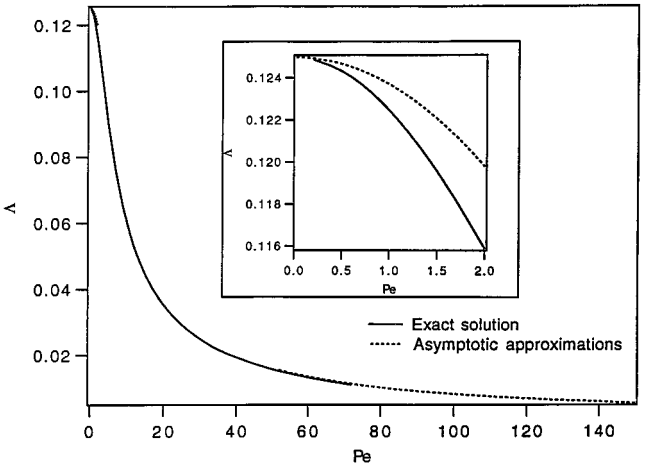

FIGURE 3 The dimensionless duration time, Λ, is plotted as a function of the Peclet number. The solid curve corresponds to the numerical values of Eq. 18; the dashed curves correspond to the asymptotes at low and high Pe. The low Pe region is shown in the inset.

Note that if $\Lambda\delta \gg 1$, the reaction is transport limited, with $P \approx 1$ and $k_f \approx k_o$. If $\Lambda\delta \ll 1$, then $P \approx \Lambda\delta$, and the reaction is reaction limited ($k_f = \pi D\mathrm{Nu}\Lambda\delta$). With increasing Pe (relative velocity) the reaction will become reaction limited. We plot the nondimensionalized rate constant k_f/D at different values of δ as a function of Pe in Fig. 4. The reaction rate increases with Pe (relative velocity) and then reaches a plateau. This indicates that convection enhances the rate of collision and hence reaction. Although the reaction rate reaches a steady value at high Pe, we note that this steady value is dictated by δ (the intrinsic reaction rate). Moreover, the asymptotic value for k_f/D is reached at lower values of Pe when δ is lower. In the next section we apply our theory to cell adhesion and compare it with the experiments by Pierres et al. (1994) and Tempelman (1993).

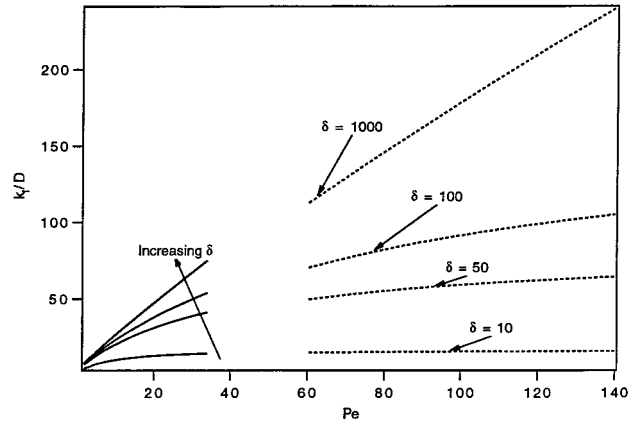

FIGURE 4 The dimensionless forward rate constant, k_f/D, is plotted as a function of Pe for four different Damkohler numbers, δ, according to Eq. 20. Dashed curves are asymptotes at high Pe.

APPLICATION TO DYNAMIC CELL ADHESION UNDER FLOW

For cells adhering to a flat surface under flow, a cell surface adhesion receptor is our target molecule on surface 1, i.e., the cell surface. We assume that this surface in the region of contact is locally flat, with a radius of the cell R much larger than the molecular length. Surface 2 is the flat substrate surface. A cut-off distance H_c is assigned to define this contact region, such that only receptors inside the contact region are able to contact and bind to the ligand on the flat surface. Thus the target molecule on surface 1 becomes active only when it is inside the contact region. This conceptualization does not require that the membrane be flat. The "contact zone" includes all receptors at the cell surface that are close enough to bind the substrate.

The relative velocity between the two surfaces, $\mathbf{V}$, can be calculated from hydrodynamic theory. Only V_x, the component parallel to the surface, is needed. Consider a cell moving with a translational velocity U in the x direction and with an angular velocity Ω in the y direction in a shear flow as illustrated in Fig. 5. The relative velocity, V_x, between the target molecule and surface 2 is the slip velocity of the sphere, $U - R\Omega$. Although the relative velocity depends on the location of the target receptor (due to the curvature of the surfaces), here we have assumed, during the time when the target receptor is in the contact region, that the relative velocity is constant. The slip velocity of the cell before the formation of a single bond is constant and only depends on the gap distance h and shear rate. In the experiments of Pierres et al. (1994) and Tempelman (1993), the translational velocities of cells at different shear rates were measured. With an estimated h/R value of 0.005, hydrodynamic theory for motion of a sphere near a wall predicts that the ratio $R\Omega/U$ is 0.53 (Goldman et al., 1967). Therefore the slip velocity is $\sim 0.47U$.

Because of cell rotation, a receptor will only be in the contact zone for a finite time. The time τ is valid only if it is smaller than the average time for a receptor to stay inside the contact zone. The average duration of a receptor inside the contact region is L_c/V_x, where L_c is on the scale of the radius of the contact region. Because $\tau/a/V_x$ is smaller than 1 for all Pe according to Eq. 18, $\tau/L_c/V_x$ is less than a/Lc. Thus the estimated value of a/L_c is ~ 0.04. Thus L_c/V_x is a much larger time than the escape time τ, and thus this calculation is unaffected by receptor rotation through the contact zone.

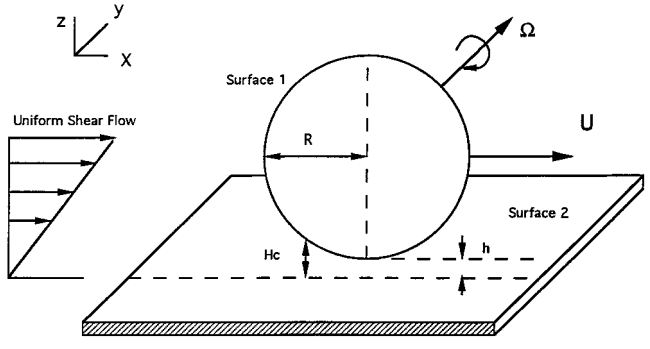

FIGURE 5 Schematic view of a cell adhering to a flat surface under flow.

Comparison to the experiment of Pierres et al.

In this work, lymphoid cells bearing CD8 molecules were driven along an anti-CD8-coated surface by a shear flow. The effect of shear rate on cell arrest frequency was studied in one set of experiments. The binding percentage (% bound) is found to decrease as the shear rate increases. Because the time needed for cells to move across the microscope field of view decreases with increasing shear rate, the intrinsic rate constant for adhesion must be deduced from the data. To compare with the theory, we first need to extract an overall or observable adhesion rate constant k_{ad} from them. Assuming the binding to be a first-order reaction, the number of bound cells N_b should obey the rate law,

$$\frac{dN_b}{dt} = k_{ad}(N_0 - N_b) \tag{21}$$

where N_0 is the total number of cells available to bind. With the initial condition $N_b(t = 0) = 0$, Eq. 21 gives $N_b(t)/N_0 = 1 - \exp(-k_{ad}t)$. In these experiments we are comparing with, the time of observation is not given explicitly. Each test cell was followed along the chamber floor until it exited the microscope field. The reaction time for a typical experiment should equal the time needed for each cell to pass through the microscope field. Given the view length L (215 μm) and cell velocity U, the percentage of cells attaching to the surface at the end of the experiment should be $1 - \exp(-k_{ad}L/U)$. Thus k_{ad} can be obtained by a simple manipulation of the binding percentage, i.e., $k_{ad} = -U/L\ln(1 - \%\ \text{bound})$. By reconstructing the % bound versus shear rate data from the work of Pierres et al. (1994), k_{ad} is plotted as a function of Pe in Fig. 6. In this calculation, the Peclet number is $0.47Ua/D$, where the receptor diffusivity D is taken to be 7.0×10^{-11} cm^2/s (Letourneur et al., 1990), and the reactive radius a is 2.0×10^{-7} cm (Springer, 1990). As shown in Fig. 6, the observable adhesion rate constant increases with relative velocity. This result should confirm qualitatively the conclusion from our analysis that the rate of adhesion can increase with increasing relative velocity. However, to assess the approximations made in our theory, we should compare quantitatively with the theory. The main objectives are to obtain the intrinsic association rate constant and the effective ligand density that give results consistent with adhesion data and to compare them with experimental values determined independently. In addition, we may elucidate whether the binding is reaction limited or transport limited.

Using the estimated values of D and a, the effective rate constant k_f for binding between receptor and ligand can be readily obtained from Eq. 20 with one parameter k_{in}. The

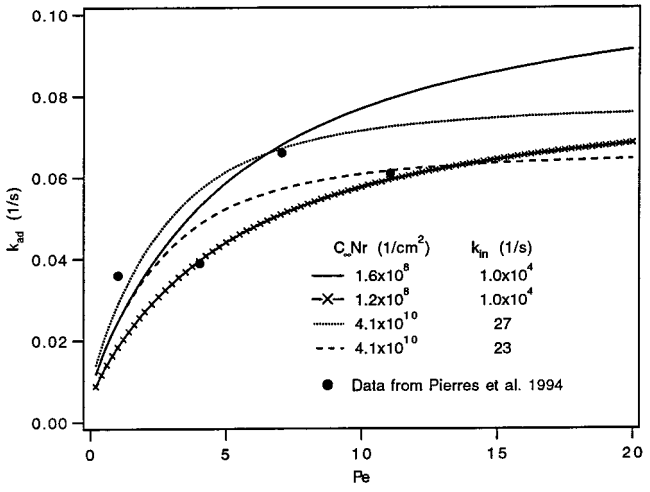

FIGURE 6 Comparison of theoretically calculated overall adhesion rate constants with the experimental values reported by Pierres et al. (1994). The two solid curves (— and -×-) give the range of $C_\infty N_r$ (1.2–1.6 × 10^8 1/cm^2) for k_{in} = 1.0 × 10^4 1/s; the dashed curve and the dotted curve mark the range of k_{in} (23.0–27.0 1/s) for $C_\infty N_r$ = 4.1 × 10^{10} 1/cm^2.

problem now is to relate k_f of a single receptor to the overall rate constant k_{ad}, which describes the rate of binding of a single cell. We assume that there is a constant number of receptors inside the contact region, N_r, available for binding. Each receptor is assumed to be independent and identical. The relation between k_f and k_{ad} can be approximated as

$$k_{ad} = k_f C_\infty N_r \tag{22}$$

where C_∞ is the surface ligand concentration. Because of the absence of sufficient data in k_{in} and N_r, we use the reported value of C_∞ (= 410 molecules/μm^2) and set N_r = 1 to obtain k_{in} by matching with the experiment. The results are shown in Fig. 6. Given these values of C_∞ and N_r, we find that values of k_{in} between 23 and 27 1/s give acceptable agreement with the adhesion data. These values are relatively low compared to typical antigen-antibody interactions (Mason and Williams, 1986). There are two possible reasons for this discrepancy. Either k_{in} is this low, because of a low value of F_s, the steric factor, or C_∞, the ligand concentration, is lower than reported. Low values of both F_s and C_∞ would have a similar origin—potential reactants present in unfavorable configurations, perhaps adversely affected by flow, reducing the potential for binding. An alternative would be to determine a value of C_∞ that gives an acceptable agreement with data at a fixed k_{in}. If $k_{in} = 10^4$ 1/s, the essential ligand concentration is 1.2–1.6 × 10^8/μm^2, ~100-fold less than the reported value (Pierres et al., 1994). Therefore to obtain good agreement between theory and experiment, we find that either the density of accessible ligand is far below that reported or that the intrinsic reaction rate is far below that found for typical antigen-antibody pairs. The idea that effective ligand density might be far below the reported value has been cited before (Kuo and Lauffenburger, 1993). An additional insight we obtain from these experiments is that $\Lambda\delta$ must be between 0.7 and 0.0003 to fit the data. Therefore $\Lambda\delta < 1$ for all combinations of parameters that give good agreement with experiment, suggesting that binding in this system is reaction limited and that most collisions between receptors and ligands will not lead to successful binding.

Comparison to the experiment of Tempelman and Hammer

In the experiments of Tempelman and Hammer (1994), adhesion was mediated by binding between cell-bound IgE and surface antigen. Rat basophilic leukemia (RBL) cells were preincubated with anti-dinitrophenol IgE antibody so that antibodies are bound to RBL cell surface Fc_ε receptors through the Fc portion of IgE. The substrate surface was prepared by covalently attaching 2,4-dinitrophenol (DNP) to a thin polyacrylamide gel. This system is well characterized in that the kinetics and affinity of binding between DNP and anti-DNP IgE have been measured (Tempelman and Hammer, 1994).

In these experiments, cells were allowed to settle on to a portion of the gel without DNP, and then cells were counted. Then buffer flow was directed into the chamber, and the cells were displaced on to the antigen-coated portion of the gel, after which the cells that bound to the gel were counted. To obtain the overall binding rate, the percentage of binding is needed. With the batch mode perfusion procedure, there is some uncertainty in the denominator of the binding percentage, i.e., the total number of cells that are available for binding, because some portion of the settled cells may be disturbed by the flow to higher streamlines, such that they will not be in contact with the bottom surface during part or all of the perfusion. However, according to the spatial pattern of the bound cells, cells stop binding to the bottom surface two to three fields of view before the end of the chamber (Tempelman, 1993); we assume that all of the bound cells are the ones have access to the bottom surface. With this assumption we can extract the overall rate constant from the spatial locations of the adherent cells.

From Eq. 21, the cumulative percentage of binding at time t is $1 - \exp(-k_{ad}t)$. Let x be the distance at which a cell has bound from the location of the non-DNP/DNP interface. The time t can be represented as x/U. Thus the cumulative percentage of binding up to position x, $B(x)$, is $1 - \exp(-k_{ad}x/U)$. A least-squares curve fit on the $\ln(1 - B(x))$ versus x plot is performed to determine k_{ad}/U. We have applied the same procedure to experiments at different shear rates to obtain the corresponding values of k_{ad}/U. Three such plots are shown in Fig. 7.

Substituting the measured cell velocities at different shear rates, we plot the calculated k_{ad} as a function of Peclet number, where $a = 10^{-7}$ cm and the lateral diffusivity D for the Fc receptor is 2 × 10^{-10} cm^2/s (Tempelman and Hammer, 1994). As illustrated in Fig. 8, the calculated k_{ad} also increases with shear rate. Using the estimated intrinsic rate

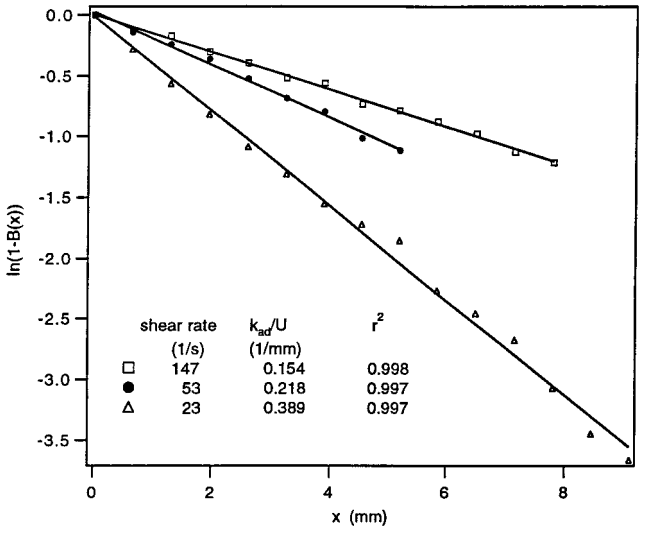

FIGURE 7 The plots of cumulative percentage adhesion, $B(x)$, for three different shear rates from measurement reported by Tempelman (1993). To obtain the overall adhesion rate constant, $\ln(1 - B(x))$ is plotted as a function of x, the distance from the interface. Slopes give the values of k_{ad}/U.

constant (4.1×10^6 1/s), the fitting result gives the product $N_r C_\infty$, $\sim 20–25 \times 10^6$ 1/cm^2. The experiment reports the product to be 1.4×10^{12} 1/cm^2 ($N_r \approx 40$, $C_\infty \approx 3.6 \times 10^{10}$ 1/cm^2) (Tempelman and Hammer, 1994), which is 10^5 larger than that required to match the result. In contrast, substituting the $N_r C_\infty$ value reported in experiment into the present theory, the theory is not able to match experiment. We suspect that because of the porosity of the gel, most DNP molecules in the gel may not be accessible to cell-bound antibodies. We find that the best match of data to our theory is for $k_{in} = 2.0 \times 10^5$ 1/s, and $N_r C_\infty = 5.0 \times 10^7$ 1/cm^2. That is, both the intrinsic reaction rate and the ligand density are smaller than reported in the original paper, to give good agreement between theory and experiment. In

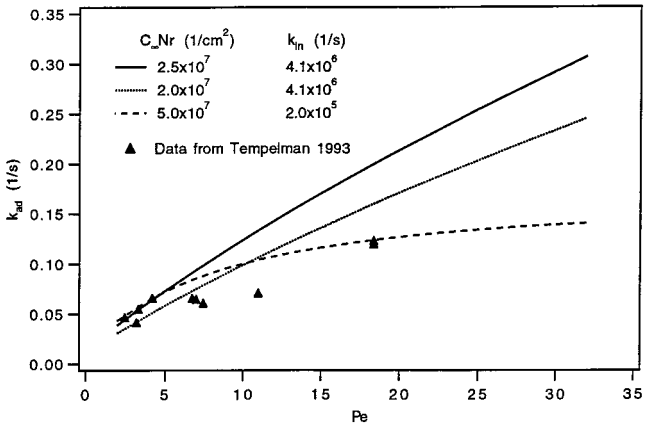

FIGURE 8 Comparison of theoretically calculated overall adhesion rate constants with the experimental values reported by Tempelman (1993). The solid curve and the dotted curve mark the range of $C_\infty N_r$ ($2.0–2.5 \times 10^7$ 1/cm^2) for $k_{in} = 4.1 \times 10^6$ 1/s.

contrast to the work by Pierres et al. (1994), the parameter $\Lambda\delta$ is > 1 and decreases from 23 to 4 as shear rate increases, indicating that the binding is transport limited. In the transport limit, the rate constant for binding increases more rapidly with Pe than in the reaction limit.

Comparison to the experiments of Wattenbarger et al.

In these experiments, the adhesion of glycophorin-coated liposomes to wheat germ agglutinin (WGA)-coated surfaces was measured in a flow chamber. The adhesion events displayed by individual liposomes were recorded. Liposomes with low glycophorin concentration were observed to stick and release many times while traveling down the chamber. The adhesion was quantified by using a sticking probability, the inverse of the number of adhesive contacts a liposome makes with the surface before it permanently adheres. The sticking probability decreases as the shear rate increases from 5 1/s to 22 1/s. However, the decrease in the sticking probability is not equivalent to a decrease in the binding rate. To determine the binding rate, we must know the average time interval between adhesive contacts, which was not given. However, after making several assumptions about how the experiments were carried out, we can come to some conclusions about the trend in the adhesion rate with shear rate.

The main assumption is that when a liposome binds permanently, it does so at the rear of the field of view. We also assume that the liposome is in contact with the surface during its entire transit during the field of view. For a sticking probability less than 1, a liposome must stop at least once before adhering permanently. For a fixed field of view, a decrease in sticking probability suggests that the liposomes travel farther between tethers. However, the distance traveled between tethers is also proportional to the shear rate. Thus, the binding rate, which is the (number of sticking events)/(mean interacting time) is proportional to the shear rate/sticking probability. (Note that the binding rate is not always proportional to this ratio, but only when subject to the constraint that the liposome must bind permanently by the end of the transit through the field of view.) For the binding rate to decrease with the shear rate, the sticking probability must be increasing faster than the shear rate. However, at shear rates of 5, 10, and 22 1/s, the ratio of shear rate to sticking probability follows the trend, 5.61, 12.5, and 48.9 1/s, respectively. Thus the apparent binding rate is increasing as shear rate increases, consistent with the qualitative predictions made in this paper.

Note that if the liposome is not in contact with the surface for the entire transit, but ultimately adheres before it leaves the field of view, the liposome must bind permanently after a shorter period of contact time with the surface as the shear rate increases. In other words, the adhesion rate will go up with shear rate more sharply than predicted above. So this assumption does not adversely affect our conclusions.

APPLICATION TO ADHESIVE DYNAMICS

Hammer and Apte (1992) developed a numerical method, adhesive dynamics, that simulates the interaction between a single cell and a ligand-coated surface under flow. In modeling adhesion, the receptor/ligand separation distance was considered to be the only factor to affect the forward reaction rate explicitly. Other factors such as diffusivity, size and orientation of the binding site, and surrounding solution are combined into a single parameter, the intrinsic rate of reaction. These calculations did not consider the effect of convection on the transport of ligand and receptors. Thus the transport was modeled assuming Pe $\approx$ 0. Clearly, given the rates of flow, Pe $\approx$ O(1–10), this effect should be incorporated into the rates of reaction. Therefore, as an improvement of the method, we have incorporated the correct rate expression into adhesive dynamics. Here we use a simpler model to describe the dependence of the forward rate on the receptor/ligand separation distance. Let d_i be the separation distance between the substrate surface and the position on the cell surface to which receptor i is attached, and H_c be a cut-off separation distance to define the reactive contact region (see Fig. 5). When $d_i \leq H_c$, the receptor i is reactive with $k_f = \pi D \mathrm{Nu}\mathbf{P}$ (Eq. 20). If $d_i > H_c$, receptor i is not reactive. Because the purpose of this work is to study the forward reaction, once a tether is formed between the cell and the surface, the cell is defined as adherent and the simulation stops. This is valid for low shear rates, such as those used by Pierres et al. (1994) and Tempelman and Hammer (1994). Otherwise, our implementation of adhesive dynamics is as before (Hammer and Apte, 1992; Chang and Hammer, 1996). Here we present a set of simulation data from this improved method. In this set of simulations, most of the parameters are the same as our previous work (Chang and Hammer, 1996). The parameters that are changed or important for this work are listed in Table 1.

For each shear rate, 100 cells are tested numerically. The percentage of cells that adhere to the surface is plotted as a function of shear rate in Fig. 9. Adhesion data shown in Fig. 9 demonstrate the commonly observed trend that adhesion percentage decreases with increasing shear rate. Thus even as the forward rate increases with increasing flow rate, the decrease in the passage time leads to a decrease in binding with flow rate. Because the forward rate increases with increasing shear, adhesion in Fig. 9 decreases only modestly with increasing shear. A flat tail has been observed in the experiment of Pierres et al. (1994) and may thus be recognized as the signature of an increasing forward rate constant with increasing shear rate. The cumulative percentage of binding up to position x, $B(x)$, for each shear rate is presented in Fig. 10. The function $1 - B(x)$ turns out to be an exponential function of $-x$. Thus the first-order reaction kinetics is preserved in our simulations.

Finally, using the adhesive dynamics simulation data generated in Figs. 9 and 10, we illustrate several methods for deducing the intrinsic adhesion rate constant k_{ad}. The results are listed in Table 2. From the parameters used in the simulations, an analytic k_{ad} for each shear rate can be obtained by multiplying $N_r C_\infty$ by the value of k_f calculated according to the analytic theory presented in this paper (Eq. 20). N_r is estimated as the average number of receptors inside the contact region (N_r = 13.1), and C_∞ is a known input to the simulations. This analytic result for k_f is given

TABLE 1 The parameters used in the simulation

Parameter	Definition	Value
R_c	Cell radius	4.5 mm
N_r	Receptor number	20,000
λ	Bond length	20 nm
H_c	Cut-off distance	30 nm
k_{in}	Intrinsic rate constant	1000 1/s
D	Surface diffusivity	10^{-10} cm^2/s
L	View length	0.1 cm
C_∞	Ligand concentration	10^8 #/cm^2

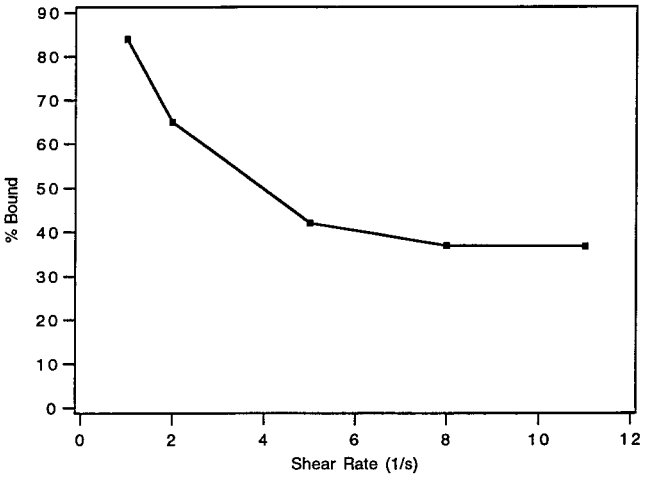

FIGURE 9 Adhesive dynamics simulation results of the total adhesion at different shear rates.

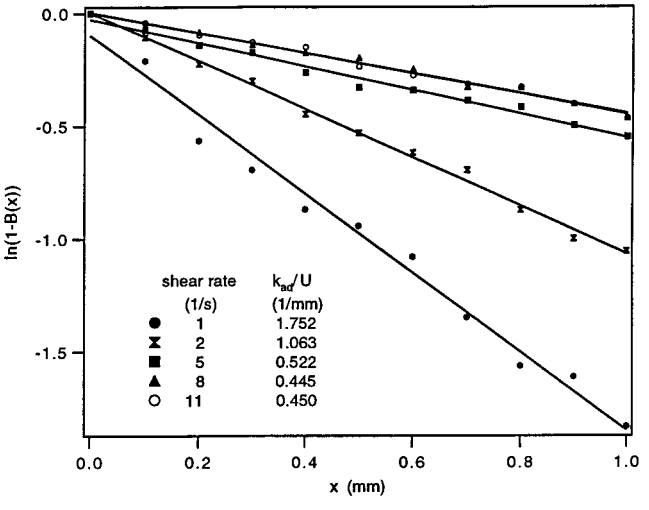

FIGURE 10 $\ln(1 - B(x))$ is plotted as a function of x for five different shear rates. $B(x)$ is the cumulative percentage of binding up to position x obtained from simulations. Slopes give the values of k_{ad}/U.

TABLE 2 Simulation results

Shear rate (1/s)	Cell velocity ($\times 10^{-4}$ cm/s)	% bound	k_{ad} (1/s) ($k_{ad} = -U/L\ln$(1-%Bound))	k_{ad} (1/s) (fit to spatial data)	k_{ad} (1/s) (analytic)
1.0	2.19	84	4.00×10^{-3}	3.83×10^{-3}	4.06×10^{-3}
2.0	4.37	65	4.59×10^{-3}	4.65×10^{-3}	4.10×10^{-3}
5.0	10.93	42	5.95×10^{-3}	5.70×10^{-3}	5.84×10^{-3}
8.0	17.48	37	8.08×10^{-3}	7.78×10^{-3}	7.38×10^{-3}
11.0	24.04	37	1.11×10^{-2}	1.08×10^{-3}	8.78×10^{-3}

in the last column of Table 2. Alternatively, k_{ad} can be extracted according to the formula $k_{ad} = -U/L\ln(1 - \%$ bound) from data on "% bound" given in Fig. 9. Both sets of k_{ad} agree well with the analytic values, except at higher shear rates, where there is statistical error due to low levels of adhesion. Therefore, there are several adequate methods at one's disposal for determining the kinetics of adhesion accurately from experimental data, and the analytic method proposed in this paper would also be quite accurate.

CONCLUSION AND DISCUSSION

A simple analysis of the motion of a cell near a surface in a hydrodynamic shear fluid indicates that at shear rates typically used in cell adhesion experiments (1 − 1000 1/s), there is a substantial convective or slip velocity in the interface between cell and surface that will affect the binding between receptor and ligand (Goldman et al., 1967). The Peclet number, which compares the effects of lateral motion of receptors to the diffusion of receptors in the plane of the membrane, is O(1) or greater, suggesting that convection is important or dominates the collision between cell surface receptors and substrate ligand. In this paper we calculated quantitatively the effect this convection has on the rate of collision and the overall rate of reaction of cell bound receptors to ligands. We illustrate that increasing the relative velocity between surfaces increases the encounter rate but decreases the collision duration, and we predict that when relative velocity increases, the forward rate constant will go up and then reach a plateau as these two effects counterbalance each other. Experimental results show a qualitative agreement with our prediction. To compare with experiments as a verification of the theory, we provide two methods to extract the rate constant for biological adhesion from experimental data. Hopefully, those methods will be useful at extracting a meaningful kinetic rate constant from adhesion experiments.

For flow chamber experiments, the quantity measured to describe cell adhesion is usually the number of cells bound per unit of time or the number of cells bound per unit time per unit area, which can be divided by the total amount of test cells to normalize the data. However, these quantities are not objective measures of the reactivity of the receptor/ligand pair. They depend on the measurement method and only provide a relative measure within the same set of experiments. For example, the percentage of cells bound, obtained by measuring the number of cells bound after a period of time divided by the total number of cells passing a specific microscope field, depends on the length of the field. Furthermore, the dependence on the length of the field cannot be removed by dividing the length of the measurement field, because binding is not linearly proportional to the length. As an alternative, the overall association rate constant k_{ad}, which must be carefully extracted from adhesion data, can serve as a proper index for the binding between cells and surfaces (Swift et al., 1998).

In this paper we have approximated the overall reaction of receptor and ligand as a two-step process involving transport and reaction. Although a transport reaction equation can be solved analogously to obtain an alternative expression of the forward rate constant, it is not as illustrative as the two-step formalism. Nevertheless, we present it for completeness in Appendix B. The two-step formalism has been used often in the past (Bell, 1978) and implies that distinct physical processes are involved in each step. However, it is easy to imagine that this compartmentalized conceptualization might break down. Specifically, one might imagine that convective transport may act to alter the shape and the orientation of the reactive molecules on a microscopic length scale in a way that alters their ability to react. In our formalism, this would correspond to a value of k_{in} that is a decreasing function of U. Calculating a priori how k_{in} might depend on U would require sophisticated molecular dynamics techniques. In comparing our method with adhesive data, we find that values of k_{in} that are smaller than measured in quiescent solution (for the same freely diffusing ligand binding to a receptor) might be needed to explain the decrease in k_{ad} with shear rate (Finger et al., 1996), which suggests that k_{in} is adversely affected by convection.

In the two-step kinetic scheme

$$R + L \underset{k_-}{\overset{k_+}{\rightleftharpoons}} R \cdot L \underset{k_{off}}{\overset{k_{in}}{\rightleftharpoons}} RL$$

our theory presents exact solutions of the encounter rate k_+ and disengagement rate $k_- = 1/t$ under the condition where the molecular transport is mediated by diffusion and convection simultaneously. The previous work that considered the effect of relative movement of receptors and ligand approximated these two rates by simply adding the contribution from diffusion to the one from convection (Potanin et al., 1993), i.e., $k_- = k_-$ (diffusion) + k_-(convection) and $k_+ = k_+$(diffusion) + k_+(convection). According to this

method, we obtain $k_+ = 2\pi D/\ln 10 + 2aV$, $k_- = 8D/a2 + 3\pi V/8a$, and $k_f = k_+k_{in}/(k_{in} + k_-)$. We compare the k_f obtained from our theory with the k_f obtained from this approximate method in Fig. 11 for $\delta = 50$. Within the experimentally and physiologically relevant range of Pe, the approximate method gives an error of ~10–20%. This is also true for other values of δ (data not shown). This error is significant, and it persists for all values of Pe. Because convection is dominant in this range of Pe, k_f is best approximated by k_f under pure convection ($D = 0$). Our theory clearly presents an accurate way to add the contribution from diffusion to the one from convection in determining the overall rate of binding.

Recently Finger and colleagues observed that shear above a critical threshold is required to promote and maintain rolling interaction through L-selectin (Finger et al., 1996). This special behavior is not seen in the neutrophil rolling on E-selectin or P-selectin, or for lymphocyte rolling on vascular cell adhesin molecule-1, where the number of rolling cells decreases with increasing shear rate (Finger et al., 1996). (Other laboratories have reported that the shear threshold is seen with some of these chemistries (Lawrence et al., 1997); thus, there is a controversy to sort out.) At low shear rates, the number of rolling cells increases with shear rate, implying that reaction in this range of shear stresses is transport-limited. Furthermore, a later study from the same laboratory demonstrated the effect of flow rate on transient tethering of lymphocytes to substrates coated with the adhesion molecule peripheral node addressin (PNAd) through the lymphocyte molecule L-selectin (Alon et al., 1997). With a lowered density of molecules on the substrate, tethering cells cannot convert to rolling. Tethering is the formation of the first bond and hence provides the most direct test of how the rate of reaction is affected by shear. It was found that the rate of initial attachment increases, then decreases with increasing shear rate. This is a direct proof that relative motion improves the binding rate. Modeling all of the shear threshold phenomena, including the decrease in tethering for higher shear stresses, requires incorporating all dynamic features that affect cell rolling, including the ligation-dependent shedding of L-selectin (Walcheck et al., 1996) and the high off-rate of L-selectin/PNAd bonds (Alon et al., 1977) and is beyond the scope of this work. However, the calculations presented in this paper provide the explanation of one key aspect of the shear threshold effect—namely, that the increase in binding with shear rate is due to transport-limited binding, in which collisions between receptors and ligands increase with increasing shear rate.

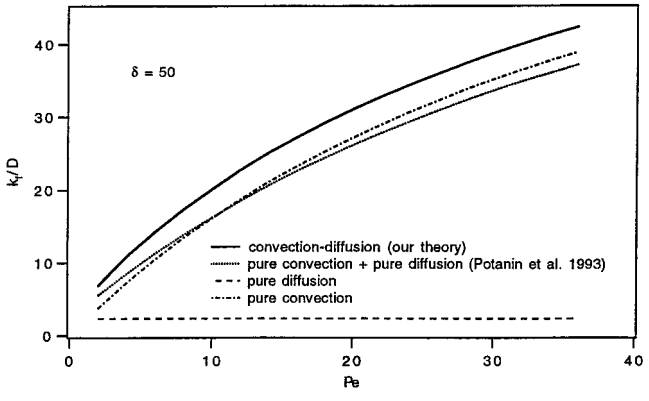

FIGURE 11 Comparison of the forward rate constant from our theory to the one from Potanin et al. (1993). The forward rates for pure convection ($D = 0$) and pure diffusion ($V = 0$) are also shown.

APPENDIX A

We present here the solution of Eq. 13. For convenience, we will replace $\langle T(\mathbf{r})\rangle$ with $Y(\mathbf{r})$ and choose $\mathbf{V}$ to be in the x direction. Equation 13 then becomes

$$V\frac{\partial Y}{\partial x} + D\nabla^2 Y = -1 \tag{A1}$$

The boundary condition becomes

$$Y(\mathbf{r}) = 0 \quad \text{at} |\mathbf{r}| = a \tag{A2}$$

A particular solution for Eq. A1 can easily be found:

$$Y_p = -x/V = -r\cos\theta/V \tag{A3}$$

Now we need to obtain the complementary solution, Y_c, which satisfies

$$V\frac{\partial Y_c}{\partial x} + D\nabla^2 Y_c = 0 \tag{A4}$$

Similar to the derivation of Eq. 5, we pursue a separation-of-variables solution. Let $H = \cos\theta$, $\kappa = V/2D$, and $G = Y_c\, e^{\kappa Hr}$. Multiplying Eq. A4 by $e^{\kappa Hr}$, we obtain

$$\frac{\partial^2 G}{\partial r^2} + \frac{1}{r}\frac{\partial G}{\partial r} + \frac{(1-H^2)\partial^2 G}{r^2\,\partial H^2} - \frac{H}{r^2}\frac{\partial G}{\partial H} - \kappa^2 G = 0 \tag{A5}$$

Seeking a solution in the form

$$G(r,\theta) = R(r)\Theta(\theta) \tag{A6}$$

we obtain two ordinary differential equations,

$$\Theta'' + \lambda^2\Theta = 0, \quad r^2R'' + rR' - \kappa^2 r^2 R - \lambda^2 R = 0$$

where λ is an arbitrary constant. The solution of the Θ equation is

$$\Theta = A\cos\lambda\theta + B\sin\lambda\theta \tag{A7}$$

Because of symmetry and the condition that $\Theta(\theta) = \Theta(\theta + 2\pi)$, the solution is now written as

$$\Theta_n = A_n\cos n\theta, \quad \text{where } n = 0, 1, 2, \ldots \tag{A8}$$

From the condition that G is finite at $r = 0$, we obtain the solution of the R equation as

$$R_n = I_n(\kappa r) \tag{A9}$$

Thus the appropriate solution of Eq. A4 is given by

$$Y_c = e^{-\kappa r\cos\theta}\sum_{n=0}^{\infty} A_n I_n(\kappa r)\cos n\theta \tag{A10}$$

And the boundary condition for Y_c is now

$$Y_c = a/V \quad \cos\theta \text{ at } r = a \tag{A11}$$

To satisfy the boundary condition,

$$\sum_{n=0}^{\infty} A_n I_n(\kappa a)\cos n\theta = a/V \cos\theta e^{\kappa a\cos\theta} \tag{A12}$$

Using orthogonality, we obtain

$$A_0 = \frac{a}{2\pi V I_0(\kappa a)} \int_0^{2\pi} \cos\theta e^{\kappa a\cos\theta} d\theta = \frac{aI_1(\kappa a)}{VI_0(\kappa a)} \tag{A13}$$

$$\begin{aligned} An &= \frac{a}{\pi V I_n(\kappa a)} \int_0^{2\pi} \cos\theta \cos n\theta e^{\kappa a\cos\theta} d\theta \\ &= \frac{a(I_{n-1}(\kappa a) + I_{n+1}(\kappa a))}{VI_n(\kappa a)} \end{aligned} \tag{A14}$$

Therefore the solution for Eq. A1 is

$$Y = Y_c + Y_p = e^{-\kappa r\cos\theta} \sum_{n=0}^{\infty} A_n I_n(\kappa r)\cos n\theta - r\cos\theta/V \tag{A15}$$

APPENDIX B

This appendix represents an alternative solution to the two-dimensional transport rate constant. We can determine a forward rate constant by solving a 2-D averaged convection-diffusion-reaction equation:

$$D\nabla^2 C - V\frac{\partial C}{\partial x} = k_{in}(r)C \tag{B1}$$

The boundary conditions are

$$C(r) = C_\infty \quad \text{at } r = \infty \tag{B2}$$

$$C(r) = \text{finite} \quad \text{at } r = 0 \tag{B3}$$

Because the reaction occurs only inside the reactive circle,

$$k_{in}(r) = 0 \quad \text{when } r > a \tag{B4}$$

$$k_{in}(r) = k_{in} \quad \text{when } r \le a \tag{B5}$$

Let $\xi = r/a$, $\kappa = Va/2D$, and $\lambda^2 = \delta + \kappa^2$, where δ is the Damköhler number. Using a method of solution similar to that described in Appendix A, we can solve Eq. B1 for the regions outside and inside the circle. For the outside region, the solution is

$$C^{(o)} = C_\infty - C_\infty\left(e^{\kappa\xi\cos\theta} \sum_{n=0}^{\infty} B_n K_n(\kappa\xi)\cos n\theta\right) \tag{B6}$$

The solution of the region inside the circle is

$$C^{(i)} = C_\infty e^{\kappa\xi\cos\theta} \sum_{n=0}^{\infty} A_n I_n(\lambda\xi)\cos n\theta \tag{B7}$$

The integration constants A_n and B_n can be evaluated by means of the two boundary conditions:

$$C^{(o)} = C^{(i)} \quad \text{at } \xi = 1$$

$$\frac{\partial C^{(o)}}{\partial \xi} = \frac{\partial C^{(i)}}{\partial \xi} \quad \text{at } \xi = 1$$

Using orthogonality, we obtain

$$A_0 = \frac{1}{\kappa K_1(\kappa)I_0(\lambda) + \lambda I_1(\lambda)K_0(\kappa)} \tag{B8}$$

$$\begin{aligned} &A_n \\ &= \frac{2(-1)^n}{\kappa(K_{n+1}(\kappa) + K_{n-1}(\kappa))I_n(\lambda) + \lambda(I_{n+1}(\lambda) + I_{n-1}(\lambda))K_n(\kappa)} \end{aligned} \tag{B9}$$

Because our goal is to obtain the total flux, J, through the reactive circle, getting the solution for the concentration field inside the circle is enough. The forward rate is related to the flux J by the expression $k_f = J/C_\infty$. Thus we can obtain a dimensionless forward rate as

$$\begin{aligned} k_f/D &= \frac{1}{C_\infty}\left(\int_0^{2\pi} \frac{\partial C}{\partial \xi} d\theta - \int_0^{2\pi} \frac{aU}{D}\cos\theta\, C\, d\theta\right) \\ &= 2\pi A_0(\lambda I_1(\lambda)I_0(\kappa) - \kappa I_1(\kappa)I_0(\lambda)) \\ &\quad + 4\pi\sum_{n=1}^{\infty}(-1)^n A_n(\lambda(I_{n+1}(\lambda) + I_{n-1}(\lambda))I_n(\kappa) \\ &\quad - \kappa(I_{n+1}(\kappa) + I_{n-1}(\kappa))I_n(\lambda)) \end{aligned}$$

This work was supported by the National Institutes of Health (HL 18208).

REFERENCES

Alon, R., S. Chen, K. D. Puri, E. B. Finger, and T. A. Springer. 1997. The kinetics of L-selectin tethers and the mechanics of selectin-mediated rolling. *J. Cell Biol.* 138:1169–1180.

Bell, G. I. 1978. Models for the specific adhesion of cells to cells. *Science*. 200:618–627.

Berg, E. L., L. A. Goldstein, M. A. Jutila, M. Nakache, L. J. Picker, P. R. Streeter, N. W. Wu, D. Zhou, and E. C. Butcher. 1989. Homing receptors and vascular addressins: cell adhesion molecules that direct lymphocyte traffic. *Immunol. Rev.* 108:5–18.

Brunn, P. O. 1981. Absorption by bacterial cells: interaction between receptor sites and the effect of fluid motion. *J. Biomech. Eng.* 103: 32–37.

Brunk, D. K., D. J. Goetz, and D. A. Hammer. 1996. Sialyl Lewis^x/E-selectin-mediated rolling in a cell-free system. *Biophys. J.* 71: 2902–2907.

Chang, K.-C., and D. A. Hammer. 1996. Influence of direction and type of applied force on the detachment of macromolecularly-bound particles from surfaces. *Langmuir.* 12:2271–2281.

Collins, F. C., and G. E. Kimball. 1949. Diffusion-controlled reaction rates. *J. Colloid Sci.* 4:425–437.

DeLisi, C. 1980. The biophysics of ligand-receptor interactions. *Q. Rev. Biophys.* 13:201–230.

Finger, E. B., K. D. Puri, R. Alon, M. B. Lawrence, U. H. von Andrian, and T. A. Springer. 1996. Adhesion through L-selectin requires a threshold hydrodynamic shear. *Nature.* 379:266–269.

Gardiner, C. W. 1990. Handbook of Stochastic Methods for Physics, Chemistry, and the Natural Sciences. Springer-Verlag, New York. 136–142.

Glaser, R. W. 1993. Antigen-antibody binding and mass transport by convection and diffusion to a surface: a two-dimensional computer model of binding and dissociation kinetics. *Anal. Biochem.* 213: 152–161.

Goetz, D. J., M. E. El-Sabban, B. U. Pauli, and D. A. Hammer. 1994. Dynamics of neutrophil rolling over stimulated endothelium in vitro. *Biophys. J.* 66:2202–2209.

Goldman, A. J., R. G. Cox, and H. Brenner. 1967. Slow viscous motion of a sphere parallel to a plan wall. II. Couette flow. *Chem. Eng. Sci.* 22:653–660.

Harlan, J. M. 1975. Leukocyte-endothelial interactions. *Blood.* 65: 513–525.

Hammer, D. A., and S. M. Apte. 1992. Simulation of cell rolling and adhesion on surfaces in shear flow: general results and analysis of selectin-mediated neutrophil adhesion. *Biophys. J.* 63:35–57.

Kuo, S. C., and D. A. Lauffenburger. 1993. Relationship between receptor/ligand binding affinity and adhesion strength. *Biophys. J.* 65:2191–2200.

Lauffenburger, D. A., and J. J. Linderman. 1993. Receptors: Models for Binding, Trafficking and Signaling. Oxford University Press, New York. 152.

Lawrence, M. B., G. S. Kansas, E. J. Kunkel, and K. Ley. 1997. Threshold levels of fluid shear promote leukocyte adhesion through selectins (CD62L,P,E). *J. Cell Biol.* 163:717–727.

Lawrence, M. B., C. W. Smith, S. G. Eskin, and L. V. McIntire. 1990. Effect of venous shear stress on CD18-mediated neutrophil adhesion to cultured endothelium. *Blood.* 75:227–237.

Lawrence, M. B., and T. A. Springer. 1991. Leukocytes roll on a selectin at physiologic flow rates: distinction from and prerequisite for adhesion through integrins. *Cell.* 65:859–873.

Letourneur, F., J. Gabert, P. Cosson, D. Blanc, J. Davoust, and B. Malissen. 1990. A signaling role for the cytoplasmic segment of the CD8 α chaion detected under limiting stimulatory conditions. *Proc. Natl. Acad. Sci. USA.* 87:2339–2343.

Luscinskas, F. W., G. S. Kansas, H. Ding, P. Pizcueta, B. E. Schleiffenbaum, T. F. Tedder, and M. A. Gimbrone, Jr. 1994. Monocyte rolling, arrest and spreading on IL-4-activated vascular endothelium under flow is mediated via sequential action of L-selectin, β_1-integrins, and β_2-integrins. *J. Cell Biol.* 125:1417–1427.

Mason, D. W., and A. F. Williams. 1986. Handbook of Experimental Immunology, Vol. 1, Immunochemistry, 4th Ed. Blackwell, Oxford. 38.1–38.17.

Melder, R. J., L. L. Munn, S. Yamada, C. Ohkubo, and R. K. Jain. 1995. Selectin- and integrin-mediated T-lymphocyte rolling and arrest on TNF-α-activated endothelium: augmentation by erythrocytes. *Biophys. J.* 69:2131–2138.

Model, M. A., and G. M. Omann. 1995. Ligand-receptor interaction rates in the presence of convective mass transport. *Biophys. J.* 69:1712–1720.

Moore, J. W., and R. G. Pearson. Kinetics and Mechanism. John Wiley and Sons, 1981. 239.

Moore, K. L., K. D. Patel, R. E. Bruehl, L. Fugang, D. A. Johnson, H. S. Lichenstein, R. D. Cummings, D. F. Bainton, and R. P. McEver. 1995. P selectin glycoprotein ligand-1 mediates rolling of human neutrophils on p-selectin. *J. Cell Biol.* 128:661–671.

Mustard, J. F., M. A. Packham, R. L. Kinlough-Rathbone, D. W. Perry, and E. Regoeczi. 1978. Fibrinogen and ADP-induced platelet aggregation. *Blood.* 52:453–466.

Myszka, D. G., X. He., M. Dembo, T. A. Morton, and B. Goldstein. 1998. Extending the range of rate constants available from BIAcore: interpreting mass transport-influenced binding data. *Biophys. J.* 72:583–594.

Nicolson, G. L. 1988. Organ specificity of tumor metastasis: role of preferential adhesion, invasion and growth of malignant cells at specific secondary sites. *Cancer Metastasis Rev.* 7:143–188.

Osborn, L. 1990. Leukocyte adhesion to endothelium in inflammation. *Cell.* 62:3–6.

Pierres, A., O. Tissot, B. Malissen, and P. Bongrand. 1994. Dynamic adhesion of CD8-positive cells to antibody-coated surfaces: the initial step is independent of microfilaments and intracellular domains of cell-binding molecules. *J. Cell Biol.* 125:945–953.

Potanin, A. A., V. V. Verkhusha, and P. V. Vrzheshch. 1993. Coagulation of particles in shear flow: applications to biological cells. *J. Colloid Interface Sci.* 160:405–418.

Purcell, E. M. 1978. The effect of fluid motions on the absorption of molecules by suspended particles. *J. Fluid Mech.* 84:551–559.

Smoluchowski, M. V. 1917. Versuch einer mathematischen theorie der koagulationskinetik kolloider losungen. *Z. Phys. Chem.* 92:129–168.

Springer, T. A. 1990. Adhesion receptors of the immune system. *Nature.* 346:425–434.

Swift, D. G., R. G. Posner, and D. A. Hammer. 1998. Kinetics of adhesion of IgE-sensitized rat basophilic leukemia cells to surface immobilized antigen in Couette flow. *Biophys. J.* 75:2597–2611.

Szabo, A., K. Schulten, and Z. Schulten. 1980. First passage time approach to diffusion controlled reactions. *J. Chem. Phys.* 72:4350–4357.

Tempelman, L. A. 1993. Quantifying receptor-mediated cell adhesion under hydrodynamic flow using a model cell line. Ph.D. thesis. Cornell University, Ithaca, NY.

Tempelman, L. A., and D. A. Hammer. 1994. Receptor-mediated binding of IgE-sensitized rat basophilic leukemia cells to antigen-coated substrates under hydrodynamic flow. *Biophys. J.* 66:1–13.

von Andrian, U. H., S. R. Hasslen, R. D. Nelson, S. L. Erlandsen, and E. C. Butcher. 1995. A central role for microvillous receptor presentation in leukocyte adhesion under flow. *Cell.* 82:989–999.

Walcheck, B., J. Kahn, J. M. Fisher, B. B. Wang, R. S. Fisk, D. G. Payan, C. Feehan, R. Betageri, K. Darlak, A. F. Spatola, and T. K. Kishimoto. 1996. Neutrophil rolling altered by inhibition of L-selectin shedding in vitro. *Nature.* 380:720–723.

Wattenbarger, M. R., D. J. Graves, and D. A. Lauffenburger. 1990. Specific adhesion of glycophorin liposomes to a lectin surface in shear-flow. *Biophys. J.* 57:765–777.

Xia, Z., H. L. Goldsmith, and T. G. M. van de Ven. 1993. Kinetics of specific and nonspecific adhesion of red blood cells on glass. *Biophys. J.* 65:1073–1083.